Journal of Sustainable Development of Energy, Water and Environment Systems

http://www.sdewes.org/jsdewes

Year 2026, Volume 14, Issue 4, 1140740

Original Research Article

Advancing the Understanding of Silver Nanoparticles Removal: Comprehensive Assessment-Based Modelling in Wastewater Treatment Plants

Paulina Vilela*[1], Gabriela-Elizabeth Vilela-Govea[2], Johanna Vanessa Zambrano Flores[3]

[1]ESPOL Polytechnic University, Escuela Superior Politécnica del Litoral, ESPOL, Facultad de Ingeniería en Ciencias de la Tierra, Campus Gustavo Galindo Km. 30.5 Vía Perimetral, P.O. Box 09-01-5863, Guayaquil 090112, Ecuador

[2]ESPOL Polytechnic University, Escuela Superior Politécnica del Litoral, ESPOL, Facultad de Ciencias Sociales y Humanísticas, Campus Gustavo Galindo Km. 30.5 Vía Perimetral, P.O. Box 09-01-5863, Guayaquil 090112, Ecuador

[3]cambiaMO, changing mobility, Calle del Duque de Fernán, 2,1ª planta, Centro, Madrid 28012, Spain

e-mail: johanna.zambrano@cambiamo.net, pvilela@espol.edu.ec, gvilela@espol.edu.ec

Cite as: Vilela, P., Vilela-Govea, G. E., Zambrano Flores, J. V., Advancing the understanding of silver nanoparticles removal: Comprehensive assessment-based modelling in wastewater treatment plants, J.sustain. dev. energy water environ. syst., 14(4), 1140740, 2026, DOI: https://doi.org/10.13044/j.sdewes.d14.0740

ABSTRACT

Silver nanoparticles discharged from wastewater treatment plants pose potential risks to aquatic environments and, in the long term, may cause serious human health issues, hindering quality of life. Limited research has been conducted, making it difficult to ensure efficient removal of silver nanoparticles in wastewater treatment plants. This study evaluates the removal efficiency of silver nanoparticles across three wastewater treatment plant layouts: conventional activated sludge, an anoxic/oxic process configuration, and a 4-stage Bardenpho process system. Silver nanoparticle removal efficiency was 82%, and nitrogen removal efficiency exceeded 95% under steady-state conditions; however, under dynamic conditions, significant efficiency reductions were observed in the Bardenpho and anoxic/oxic configurations. The results also showed variability in organic matter and nitrogen removal due to reduced internal recirculation flowrates. The findings highlight the need to optimise certain configurations to ensure balanced performance across all pollutants.

KEYWORDS

Benchmark simulation, Emerging contaminants, Silver nanoparticle removal, Wastewater treatment modelling, Wastewater treatment plants.

INTRODUCTION

The accelerated pace of industrial development, while addressing growing societal demands, has also intensified environmental degradation, influencing the discharge of untreated wastewater containing synthetic dyes, heavy metals, and other hazardous substances [1]. Silver nanoparticles (AgNPs) have become key ingredients in a wide range of consumer products [2], including medical devices, textiles, and electronics, owing to their unique antimicrobial properties and versatile applications [3]. They have physicochemical traits that, combined with their versatility, allow their incorporation into a wide array of

* Corresponding author

consumer products [4]. Their efficacy in inhibiting microbial growth and even viral activity positions them as promising alternatives to conventional antibiotics [5]. Recently, they have been studied as an added nanomaterial to enhance wastewater treatment [6]. The biological activity and functional performance of AgNPs are governed by multiple factors, such as particle size and shape, composition, surface chemistry, capping agents, dissolution rate, agglomeration state, and ion release behaviour in aqueous environments [3]. This dual nature, both therapeutic and potentially hazardous, turns them into emerging contaminants that need the development of better comprehensive toxicity assessments [7]. However, their increasing prevalence has raised significant concerns about the potential risks they pose to human health and the environment [8].

AgNPs often bypass conventional wastewater treatment plants (WWTPs) [9], potentially disrupting microbial communities that are essential to maintaining wastewater treatment efficiency [10]. This phenomenon poses a threat to the stability and efficiency of wastewater treatment plants [11], particularly by disrupting microbial communities, which are vital for pollutant degradation [12]. Although AgNPs are increasingly employed in water remediation strategies [6], their persistence and interactions within treatment systems remain poorly understood [13]. For instance, studies show that AgNPs in WWTP sludge can have negative effects, causing biotic stress and settling performance issues. Given that bacteria in WWTPs coordinate suspension and diffusion growth, the AgNP concentration alters this behaviour, leading to deterioration of the sludge floc structure [14]. Similarly, AgNPs have been shown to accumulate in the WWTP sludge, where at least 90% of the nanoparticle content is retained [15]. However, the behaviour of AgNPs in the main treatment line of WWTPs remains insufficiently understood, and few studies have been conducted to date. The persistence of remaining AgNPs in wastewater systems underscores the urgent need for a deeper understanding of their environmental behaviour and effects in WWTPs.

Over the past decades, mathematical modelling has been utilised to understand and design WWTPs. Activated sludge models (ASMs), developed by the International Water Association (IWA), have been widely adopted in literature to simulate biological nutrient removal processes [16]. These models can represent the complex microbial interactions and physicochemical processes encountered in WWTPs, allowing effective analysis of system behaviour [17]. Consequently, process modelling to study removal treatment efficiency, WWTP design, and the fate of contaminants, and the Benchmark simulation frameworks, such as the Benchmark Simulation Model No. 1 (BSM1), have been further implemented [18]. Several studies have applied ASM and BSM modelling to analyse treatment performance and evaluate control strategies in WWTPs. For instance, ASM was used to reproduce the performance of industrial and municipal WWTPs and to optimise operational conditions [19], and BSM1 was used to evaluate advanced control strategies under dynamic influent conditions [20]. The integration of emerging contaminants represents a relevant research direction for assessing contaminant fate and potential impacts without the limitations of full-scale studies.

Regarding the AgNP role in WWTP operation, studies have shown that nitrogen removal is influenced by these particles [21], indicating that AgNPs affect biological treatment efficiency [22]. In addition, most AgNPs adsorb onto sludge particles, which may further influence microbial performance and system stability [23]. More studies suggest that while AgNPs can be partially removed through biological treatment processes such as activated sludge [5], their removal efficiency depends on several parameters, including particle properties, contact time, solution chemistry, and the presence of extracellular polymeric substances (EPS) [24]. Previous research has also highlighted this importance and identified representative mechanisms of AgNPs (adsorption-desorption, inhibition, dissolution, and chemical precipitation) [25], and has applied them to an activated sludge model (ASM-AgNP) [26]. Different AgNPs sizes and influent concentrations were considered, demonstrating good removal efficiency for all parameters, including nitrogen, chemical oxygen demand, and AgNPs characteristics [26]. Considering that particle characteristics

and fate mechanisms may be directly related to the treatment conditions of WWTPs, the present study investigates removal efficiency in plants using the ASM-AgNP model across different WWTPs to expand understanding of AgNP removal.

Despite numerous investigations on the effects of AgNPs on microbial communities and biological treatment, limited research has been conducted on their influence across varied WWTP configurations, accounting for physical conditions and treatment lines, and on their most well-known fate mechanisms, such as adsorption, dissolution, and inhibition. Given these challenges, it is essential to understand how different wastewater treatment plant configurations manage AgNP concentrations and how they influence biological treatment performance. This study aims to (i) assess the removal efficiency of AgNPs and nitrogen species using the ASM-AgNP modelling; (ii) compare the performance in three wastewater treatment plant configurations under steady state and dynamic conditions: Benchmark Simulation Model No. 1 (BSM1), Bardenpho process, and Anoxic/Oxic (A/O) process; and (iii) evaluate the influence of system configuration on treatment efficiency and effluent quality. By employing dynamic modelling, this research seeks to evaluate treatment strategies and conditions, and to contribute to a better understanding of the environmental behaviour of AgNPs in wastewater treatment infrastructure. The study's structure includes an introduction that presents the major fundamentals and objectives, a methodology that describes the models and the equations used, results and discussion that describe the evaluation of the results, and, finally, the conclusions.

MATERIALS AND METHODS

This study adopts a schematic research framework to model a wastewater treatment system, focusing on biological treatment using the activated sludge process. The modelling was performed under steady-state and dynamic conditions. The activated sludge model with silver nanoparticles (ASM-AgNP) from Vilela et al. [26] is used as a base model, already validated for WWTPs within the BSM1 and the activated sludge model No. 1 (ASM1). The effluent quality is evaluated using the following parameters: chemical oxygen demand (COD), biological oxygen demand (BOD), nitrite (NO_2^-), nitrate (NO_3^-), ammonia nitrogen (NH_4^+-N), and total nitrogen (TN). The following sections explain the further steps taken within the development of this study and the dynamic simulations.

Evaluation Framework

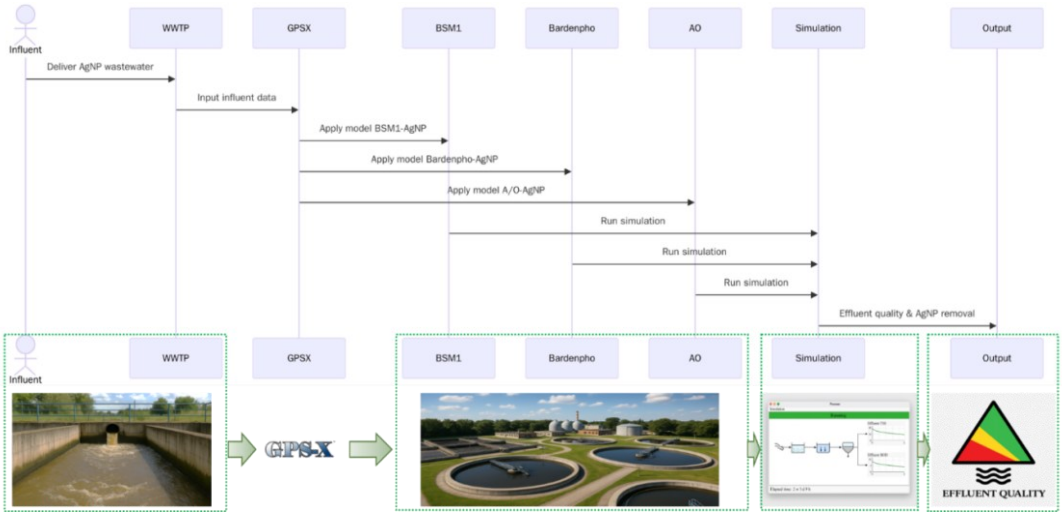

Figure 1. Sequence-wise framework of the study

The study's framework is presented in **Figure 1**. It illustrates the methodology for analysing the behaviour of AgNPs in WWTPs through the simulations of the ASM-AgNP within the BSM1 (BSM1-AgNP), Bardenpho 4-stage model (Bardenpho-AgNP), and the anoxic/oxic model (A/O-AgNP). Furthermore, the removal efficiency of AgNPs is evaluated in the WWTP layouts and compared to the baseline BSM1 without AgNPs. The ASM-AgNP model was developed by Vilela et al. [26], based on the conditions established by the International Water Association (IWA) [18]. The variables and process rates used in this model are presented in **Figure 2**.

		Variables																	
No.		1	2	3	4	5	6	7	8	9	10	11	12	13	14	15	16	17	18
	Process	Soluble undegradable organics	Soluble biodegradable organics	Particulate undegradable organics	Particulate biodegradable organics	Active heterotrophic biomass	Active autotrophic biomass	Particulate undegradable endogenous products	Dissolved oxygen	Nitrate and nitrite	Ammonia (NH_4 + NH_3)	Soluble biodegradable organic N	Particulate biodegradable organic N	Alkalinity	AgNP in liquid phase	Dissolved AgNP (Ag ion)	Particulate AgNP	Sodium hydroxide	Particulate Ag
		S_I	S_S	X_I	X_S	X_{BH}	X_{BA}	X_P	S_O	S_{NO}	S_{NH}	S_{ND}	X_{ND}	S_{ALK}	*Sag*	*Sdag*	*Xag*	*NaOH*	*Xpag*
1	Aerobic growth of heterotrophs		-1.4925			1			-0.492537		-0.086			-0.006143					
2	Anoxic growth of heterotrophs		-1.4925			1				-0.17238	-0.086			0.006171					
3	Aerobic growth of autotrophs						1		-18.04761	4.16666	4.252667			-0.601381					
4	Decay of heterotrophs				0.92	-1		0.08					0.0812						
5	Decay of autotrophs				0.92		-1	0.08					0.0812						
6	Ammonification of soluble organic nitrogen										1	-1		0.071429					
7	Hydrolysis of entrapped organics		1		-1														
8	Hydrolysis of entrapped organic nitrogen											1	-1						
9	Adsorption of AgNP to biomass														-1		1		
10	Desorption of adsorbed AgNP														1		-1		
11	Dissolution of AgNP to Ag ion														-1	1			
12	Chemical precipitation of Ag ion															-1		-1	1

Figure 2. ASM-AgNP model's Petersen matrix, adapted from Vilela et al. [26]

Suitable coefficients and process rates for the removal mechanisms were determined and calculated in [26], where the authors performed a system analysis and validated the model's response to varying nanomaterial influent concentrations. The model also includes chemical precipitation to enhance AgNP removal efficiency and NaOH precipitation to facilitate easy solid-liquid separation [27], enabling comparisons with previous work.

Model Development

This study used GPS-X version 8.0.1 software for technical and qualitative analyses of the baseline model BSM1 without AgNPs and three WWTP configurations mentioned in the preceding section.

Table 1. Operational parameters and characteristics of the WWTP model configurations; ano – anoxic, aer – aerobic, Bard – Bardenpho, * controlled in final reactor

Parameter	Conditions based on			
	BSM1	BSM1-AgNP	Bard-AgNP	A/O-AgNP
Influent flowrate *Q*	18,446 m³/d			
Sludge ret. time *SRT*	10 days			
Return activ. sludge RAS	18,446 m³/d			
Waste activ. sludge WAS	385 m³/d			
Dissolved oxygen *DO*	2.0 [mg/L] aerobic zones*	2.0 [mg/L] aerobic zones		

Parameter	Conditions based on			
	BSM1	BSM1-AgNP	Bard-AgNP	A/O-AgNP
Temperature	~20 °C typical		20 °C	
Internal recycle (range)	0–5Q, typical 3Q	3Q	3Q	-
Number of reactors	5-stage (2 ano + 3 aer)	5-stage (2 ano + 3 aer)	4-stage Bard (2 ano + 2 aer)	2-stage A/O (1 ano + 1 aer)

The model development follows the tool of the model developer from the software. The stoichiometry and kinetics of the ASM-AgNP model were implemented and generated using the model developer tool. Furthermore, the operational parameters and characteristics are summarised in **Table 1** following the standard BSM1 framework to ensure comparability. The influent characteristics, flowrate, sludge retention time, aeration, and sludge were maintained. The primary differences among the studied configurations are the physical configuration and the internal recycle flowrate, with BSM1 as the baseline. These variations in hydraulic and process design are critical factors influencing nutrient removal and organic matter degradation.

The key dimensions of the suggested approach are as follows: First, the ASM1-AgNP model is configured in GPS-X; second, the BSM1-AgNP, Bardenpho-AgNP and A/O-AgNP models are developed; third, the influent/sludge characteristics and operating parameters of the biological model are calibrated to the base model; fourth, the validity of the steady and dynamic simulations is evaluated on every model. The different configurations developed in GPS-X are presented in **Figure 3**.

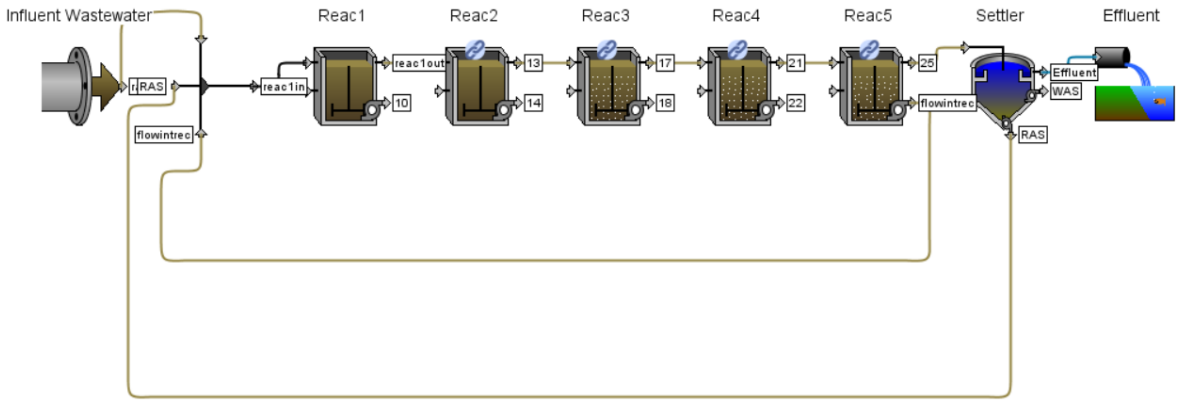

(a)

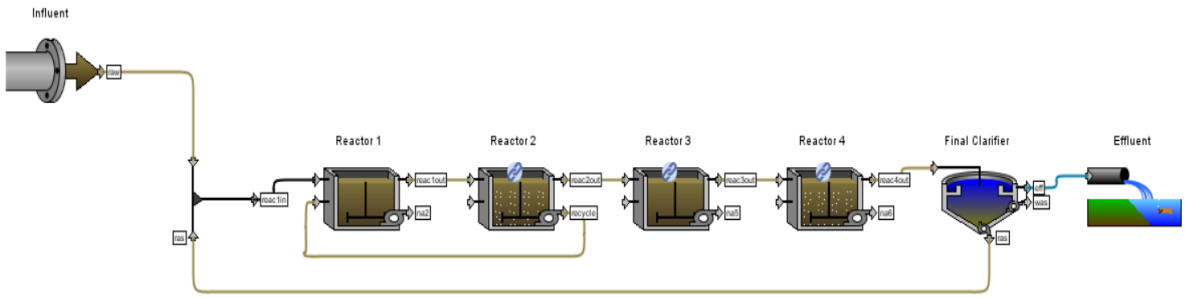

(b)

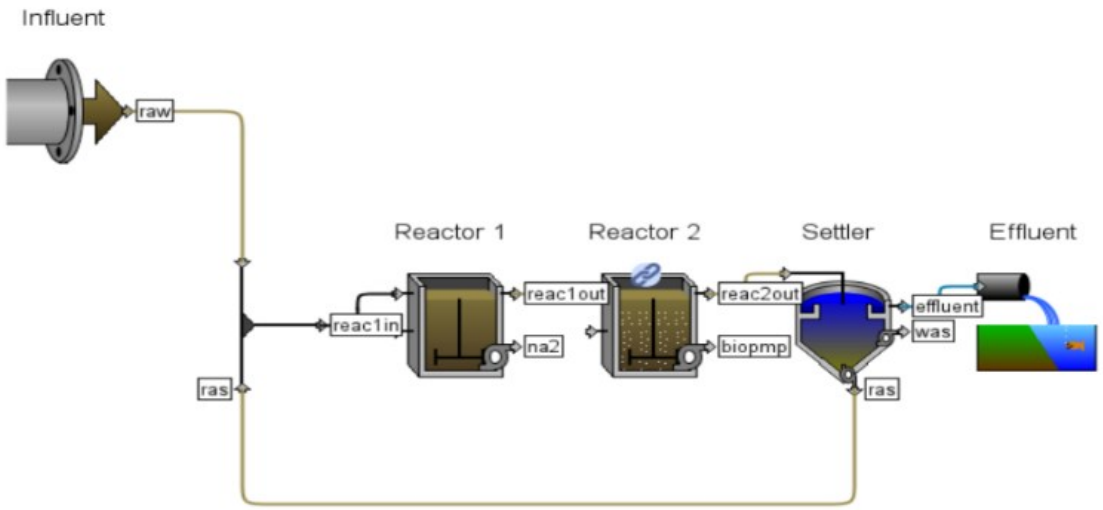

(c)

Figure 3. Wastewater treatment plant configurations evaluated in this study: BSM1 with AgNP (BSM1-AgNP) (a), Bardenpho 4-stage model with AgNP (Bardenpho-AgNP) (b), and A/O model with AgNP (A/O-AgNP) (c); the diagrams were taken from GPS-X

The dynamic simulations were performed according to the standard BSM1 dynamic conditions described by Alex *et al.* [18]. The simulation time is 14 days, and the results are analysed at the end of the simulation period. The initial phase of the simulation describes the system's stabilisation; thus, the performance evaluation focuses on the end of the simulation period.

Furthermore, the influent concentrations were primarily adopted from the BSM1 report [18], and the AgNP concentrations utilised in the WWTP models were 14.92 mg/L for AgNPs and 72.24 mg/L for Ag ion, adopted from the study of Cervantes-Avilés *et al.* [28]. The same value of 14.92 mg/L was used in all configurations, enabling a direct comparison of the calculated removal efficiencies. The influent AgNP concentration represents a worst-case scenario, with high nanomaterial levels used to evaluate system robustness rather than typical environmental conditions. Although typical environmental concentrations of AgNPs are generally reported at lower levels, higher concentrations were used to evaluate the robustness and sensitivity of the treatment configurations. This approach allows assessment of system behaviour, potential inhibitory effects, and removal performance. Given the scarcity of research and the difficulty of conducting large-scale experiments, these data have been fully adopted from published works. Hence, to partially overcome this limitation, comparisons with BSM1 without AgNPs, the baseline model, are made to analyse the validity of the results from the models. The stoichiometric processes that the model implemented for AgNP, adapted from [21] and [22], come from the mass balances presented in equations (1) to (4).

Adsorption of AgNP to biomass:

$$S_{ag} + (X_{BH} + X_{BA}) \rightarrow X_{ag} \quad (1)$$

Desorption of adsorbed AgNP:

$$X_{ag} \rightarrow S_{ag} + (X_{BH} + X_{BA}) \quad (2)$$

Dissolution of AgNP to Ag ion:

$$AgNP^0 + \frac{1}{4}O_2 + H^+ \rightarrow 2Ag^+ + \frac{1}{2}H_2O \quad (3)$$

Chemical precipitation of Ag ion:

$$Ag_2O + 2Na^+ + 2H^+ + \frac{1}{2}O_2 \rightarrow 2Ag^+ + 2NaOH \quad (4)$$

where S_{ag} is the AgNP [mg/L], $X_{BH} + X_{BA}$ represents the biomass [mg *COD*/L], and X_{ag} is the adsorbed AgNP [mg/L]. The remaining symbols denote concentrations [mg/L] of: $AgNP^0$ – silver, Ag^+ – silver ion, O_2 – oxygen, H^+ – hydrogen, H_2O – water, Na^+ – sodium, and $NaOH$ – sodium hydroxide.

Performance Assessment in Wastewater Treatment Plant Configurations

The effluent quality assessment is performed in accordance with the BSM1 report, firstly, given that the ASM-AgNP was derived from it. The conditions for the evaluation were: total nitrogen (*TN*) should be less than 18 mg/L, total chemical oxygen demand (COD_t) less than 100 mg/L, nitrogen ammonia less than 4 mg/L, and BOD_t less than 10 mg/L [18]. In addition, the effluent quality index (*EQI*) has been used to assess the quality of removal achieved by each WWTP configuration. Equation (5) shows the *EQI* calculation and the variables considered for this analysis [18].

$$EQI = \frac{1}{T * 1000}\int_{7d}^{14d}\begin{pmatrix} b_{SS} * SS_{eff}(t) + b_{COD} * COD_{eff}(t) + b_{Nkj} * S_{Nkj,eff}(t) + \\ b_{NO} * S_{NO,eff}(t) + b_{BOD5} * BOD_{eff}(t) \end{pmatrix} Q_{eff}\,(t) * dt \quad (5)$$

where b_i are the weighting factors assigned to each variable, and the concentrations of the variables are taken in [g/m^3]. All the b_i values have been adopted from the BSM1 report, namely b_{SS} = 2, b_{COD} = 1, b_{NKj} = 30, b_{NO} = 10, b_{BOD5} = 2 [18]. Furthermore, each of the variables expressed by equations (6) to (9) represents the sum of the different variables in the model at the effluent:

$$S_{Nkj,eff} = S_{NH,eff} + S_{ND,eff} + X_{ND,eff} + I_{XB}\left(X_{BH,eff} + X_{BA,eff}\right) + I_{XP}\left(X_{P,eff} + X_{i,eff}\right) \quad (6)$$

$$SS_{eff} = 0.75\left(X_{S,eff} + X_{I,eff} + X_{BH,eff} + X_{BA,e} + X_{P,eff}\right) \quad (7)$$

$$BOD_{5,eff} = 0.25\left(S_{S,eff} + X_{S,eff} + (1 - f_P).\left(X_{BH,eff} + X_{BA,eff}\right)\right) \quad (8)$$

$$COD_{eff} = S_{S,eff} + S_{I,eff} + X_{S,eff} + X_{I,eff} + X_{BH,eff} + X_{BA,eff} + X_{P,eff} \quad (9)$$

where the subscript *eff* signifies the values representing concentration in the effluent. $S_{Nkj,eff}$ is the Kjeldahl nitrogen in the effluent concentration, which is the sum of the soluble and particulate nitrogen in the model; SS_{eff} is the suspended solids of the effluent concentration; $BOD_{5,eff}$ is the *BOD* concentration at the effluent; and COD_{eff} is the effluent concentration of *COD*.

Furthermore, removal efficiencies were calculated following standard procedures. Constant influent concentrations from the BSM1 were used for steady-state conditions. For dynamic state conditions, removal efficiencies were calculated based on the average influent concentrations over the evaluation period. For AgNPs, removal efficiency is defined based on total AgNP concentration, including both soluble and particulate fractions considered in the model. Two removal approaches are considered: first, overall removal, which accounts for total mass removal and sedimentation; second, removal calculated from the effluent AgNP concentration, estimated with the influent and effluent in the liquid phase. Eq. **(10)** is used to estimate the removal efficiency.

$$RemEff(\%) = \left(\frac{C_{in} - C_{eff}}{C_{in}}\right) x100 \tag{10}$$

where C_{in} and C_{eff} represent the influent and effluent concentrations [mg/L].

RESULTS AND DISCUSSION

This section presents all the results and discussion from the performed study. The results are presented by categories, divided into sub-sections, as follows.

Removal in Wastewater Treatment Plants for the Steady State

Figure 4 shows the results obtained at the effluent from the models' simulations with base influent conditions (BSM1) for steady-state operation.

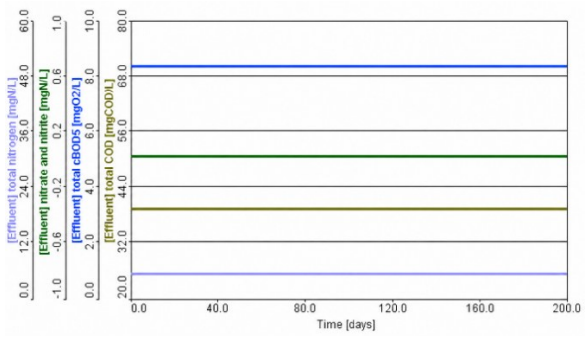

(a)

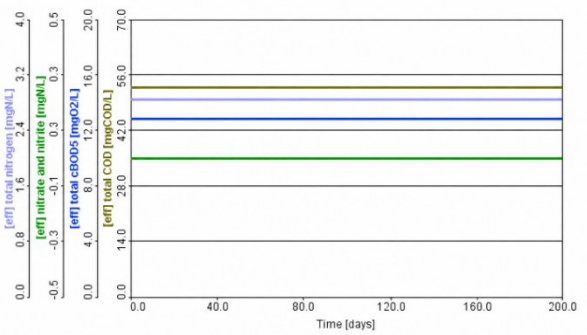

(b)

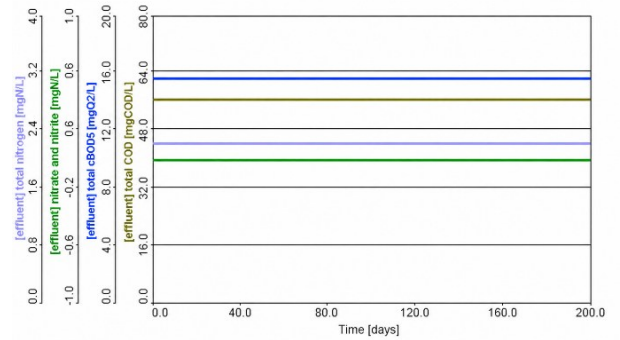

(c)

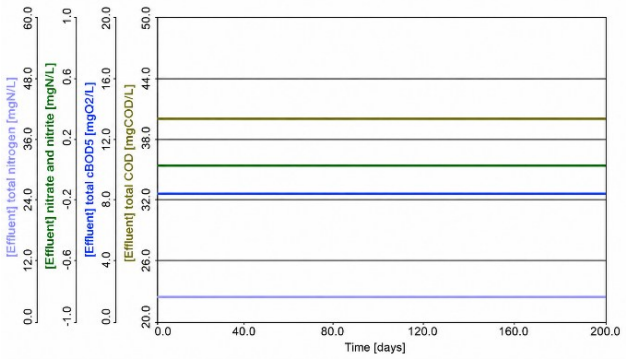

(d)

Figure 4. Effluent concentrations for steady state conditions in the models: BSM1-AgNP (a), Bardenpho-AgNP (b), A/O-AgNP (c), and BSM1 without AgNPs as the baseline configuration (d)

The concentrations of total nitrogen (*TN*), nitrate/nitrite nitrogen (NO_3/NO_2), total biochemical oxygen demand (BOD_t), and total chemical oxygen demand (COD_t) are shown. **Figure 4a** corresponds to a *TN* value of 4.57 mg/L, NO_3/NO_2 value of 0.034 mg/L, BOD_t value of 7.53 mg/L, and COD_t value of 46.11 mg/L, from the BSM1-AgNP model. These values fall within the range of the simulation results for the BSM1 model. The total *COD* shows a slightly higher value than that from the base BSM1; however, this might be related to differences in the estimation method used in the simulation software GPS-X **[29]**. It is known that the software can produce some differences in decimal places when calculations are shortened in some instances **[30]**.It should be noted that the values presented in the figures are approximate graphical representations. In contrast, the numerical values reported in the text correspond to the exact simulation outputs obtained from GPS-X.

Compared to the baseline BSM1 without AgNPs (**Figure 4d**), the model yielded results similar to those, with final effluent concentrations around the same values, differing by a few decimal places; for instance, COD_t was 39.1 mg/L, and *TN* was 5.33 mg/L in the BSM1. The major highlight is that the *TN* concentration in the BSM1-AgNP is slightly lower than in the BSM1, indicating similar removal for both. Moreover, for AgNPs, a high removal was observed, obtaining an average effluent concentration of 2.7 mg/L for all the WWTP configurations, as shown in **Figure 5** (next page), and it did not interfere with the removal of the rest of the components considered in this analysis, such as *TN*, *COD*, and *BOD*.

Following the analysis, **Figure 4b** shows *TN* at 2.22 mg/L, NO_3/NO_2 reaching zero, BOD_t value at 12.85 mg/L, and COD_t value at 52.79 mg/L from the Bardenpho-AgNP model. Finally, **Figure 4c** shows that, according to the A/O-AgNP model, the *TN* value was 2.85 mg/L, NO_3/NO_2 reached 0, BOD_t was 15.65 mg/L, and COD_t was 56.56 mg/L. For these two model configurations, the results show higher *COD* concentrations, which are related to the physical conditions of fewer reactors and lower or absent internal recycle flowrates. This provides insight into the influence of the recycle flowrate on *COD* removal efficiency in wastewater treatment plants. Moreover, the BSM1 model without AgNP concentration yielded final values of COD_t 39.1 mg/L

and *TN* 5.33 mg/L, as shown in **Figure 4d**, indicating that *TN* removal was higher and COD removal was lower compared to the Bardenpho-AgNP model. Similarly, comparing the Bardenpho-AgNP model, the *TN* was lower, and the COD_t was slightly higher within the same range, both showing good removal in this configuration. Meanwhile, for the A/O-AgNP model, *TN* also had a low value and a smaller increase in COD_t than in the BSM1 results. Hence, both configurations show good removal results. In general, both configurations showed similar behaviour for steady-state conditions.

Table 2 summarises the steady-state performance of the WWTP configurations, integrating effluent concentrations, removal efficiencies, and *EQI* values.

Table 2. Overall results for steady state conditions corresponding to effluent-based removal

Configuration	*TN* [mg/L]	*TN* removal [%]	*COD* [mg/L]	*COD* removal [%]	*BOD* [mg/L]	*BOD* removal [%]	AgNP [mg/L]	AgNP removal [%]	*EQI* [kg·units/d]
BSM1-AgNP	4.57	84.8	46.11	84.6	7.53	96.2	~2.7	>81	5455
Bardenpho-AgNP	2.22	92.6	52.79	82.4	12.85	93.6	~2.7	>81	11310
A/O-AgNP	2.85	90.5	56.56	81.1	15.65	92.2	~2.7	>81	13700

It is noted that removal efficiencies were calculated based on influent and effluent concentrations, in agreement with the values presented in the figures and tables. For AgNPs, the reported percentages correspond to effluent-based removal, consistent with the observed concentration reduction, accounting for combined soluble and particulate AgNPs in the model. The results indicate that all configurations achieved high treatment efficiencies, particularly for *BOD* removal, exceeding 90%, especially in the BSM1-AgNP configuration. Nitrogen removal efficiencies were also consistently high, whereas *COD* removal was lower in the Bardenpho-AgNP and A/O-AgNP configurations. The *EQI* results further confirmed that the BSM1-AgNP configuration provides the best overall effluent quality. Higher *EQI* values represent a relation to increased residual organic matter in the effluent.

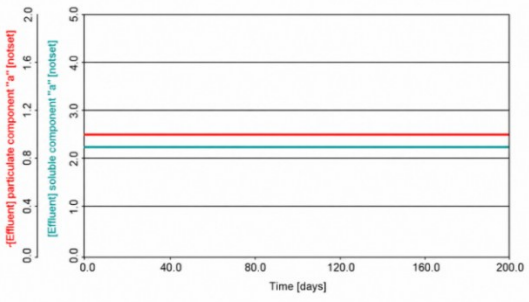

(a)

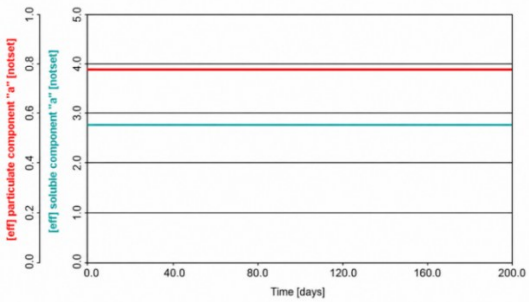

(b)

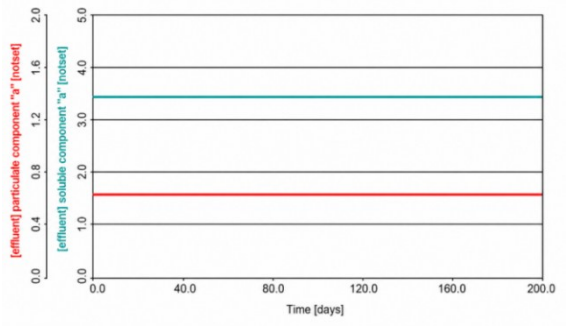

(c)

Figure 5. Effluent AgNP concentrations for steady state conditions, where soluble component "a"represents AgNP and particulate component "a" represents particulate AgNP in the models: BSM1-AgNP (a), Bardenpho-AgNP (b), and A/O-AgNP (c)

Overall, as shown in **Figure 6**, steady-state removal efficiencies were estimated relative to the standard BSM1 baseline. *BOD* removal exceeded 90% in all configurations, with the highest value in the BSM1-AgNP configuration at approximately 96%. This removal may indicate strong biodegradation under stable conditions. Nitrogen removal efficiencies were 85% in BSM1-AgNP and over 92% in the Bardenpho-AgNP configuration, suggesting enhanced denitrification processes. Furthermore, *COD* removal was slightly lower, 81% and 85%, in the Bardenpho and A/O configurations, respectively. This result might be related to the low internal recirculation flowrate and the number of reactors per configuration. The steady-state results show that all configurations provide robust treatment performance, especially BSM1-AgNP, with a more stable removal efficiency across all parameters.

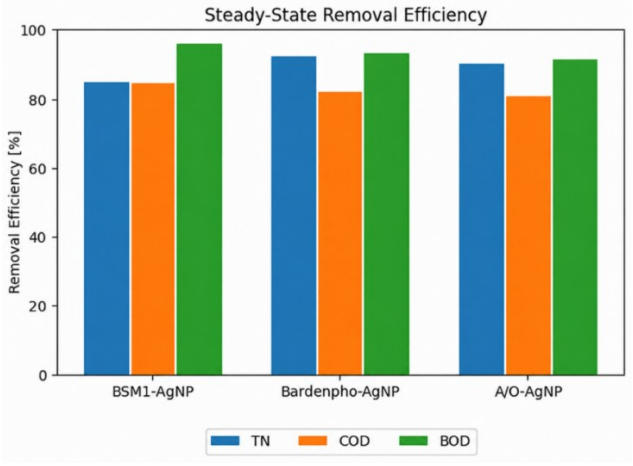

Figure 6. Removal efficiencies in steady state for the BSM1-AgNP, Bardenpho-AgNP, and A/O-AgNP models

Removal in Wastewater Treatment Plants for the Dynamic State

The results for AgNP concentrations under dynamic conditions (AgNP and particulate AgNP) are shown in **Figure 7**, which shows similar behaviour and an average value of 2.2 mg/L. Moreover, **Figure 8** shows the results from the models' dynamic simulations. **Figure 8a** corresponds to a TN value at 14 days of 11.34 mg/L, NO3/NO2 value at 14 days of 0.68 mg/L, BODt value at 14 days of 6.03 mg/L, and CODt value at 14 days of 43.04 mg/L, from the BSM1-AgNP. The TN and BOD values are slightly different, being lower and higher than those reported in the BSM1 report, respectively. This result might be related to the stoichiometric and physical conditions of the model. Furthermore, **Figure 8b** corresponds to a TN value at 14 days of 26.68 mg/L, NO3/NO2 value at 14 days of 0.053 mg/L, BODt value at

14 days of 11.18 mg/L and CODt value at 14 days of 49.83 mg/L, from the Bardenpho-AgNP. The values of TN, BOD, and COD are higher than those described in the BSM1 report and the BSM1-AgNP. However, this did not affect the model's performance simulation. Furthermore, the BSM1 model without the AgNPs final effluent concentration values, for dynamic conditions, of CODt 35.07 mg/L and TN 5.81 mg/L, as presented in **Figure 8d**, which compared to the BSM1-AgNP model, represents a lower value, indicating that the removal of nitrogen and COD was not as good in the BSM1-AgNP. Compared to the Bardenpho-AgNP, the results are consistent with previous observations; *TN* and *COD* were less removed, with a small difference. Finally, **Figure 8c** corresponds to a *TN* value at 14 days of 32.2 mg/L, NO_3/NO_2 value at 14 days of 0.022 mg/L, BOD_t value at 14 days of 14.69 mg/L, and COD_t value at 14 days of 54.74 mg/L, from the A/O-AgNP model.

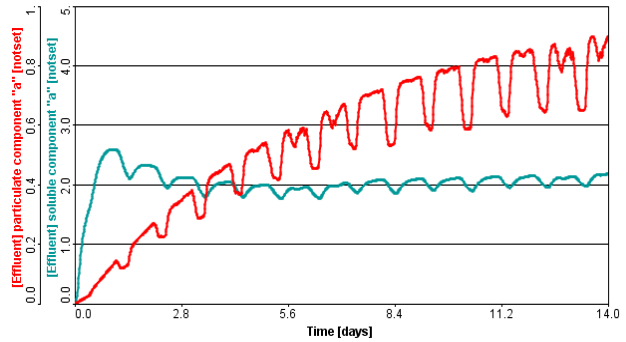

(a)

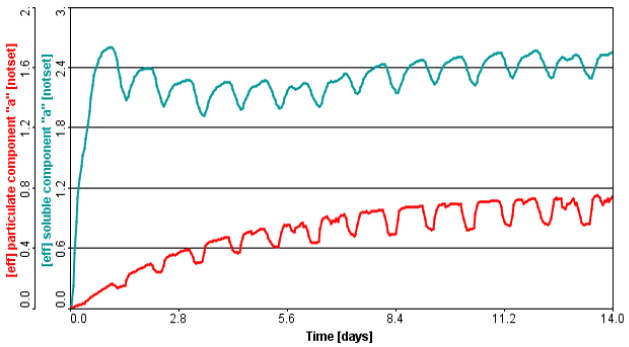

(b)

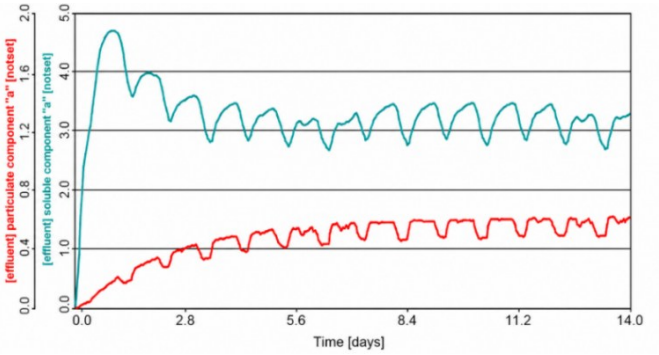

(c)

Figure 7. Effluent AgNP concentrations for dynamic conditions, where soluble component "a" represents AgNP and particulate component "a" represents particulate AgNP in the models: BSM1-AgNP (a), Bardenpho-AgNP (b), and A/O-AgNP (c)

Compared to the BSM1-AgNP, the results show higher effluent concentrations for all components. BSM1 describes dynamic results of average *TN* 15.57 mg/L, BOD_t 2.77 mg/L, and COD_t 48.30 mg/L **[18]**. Compared to these values, the results obtained with the BSM1-AgNP

model fell within a range, accounting for differences in the software's decimal precision. The Bardenpho-AgNP model results showed higher *TN* in the effluent, a more substantial increase in BOD_t, but with a COD_t value within the same range. Compared to the BSM1 model without AgNPs, the final concentration values (COD_t 35.07 mg/L and *TN* 5.81 mg/L) were lower, as shown in **Figure 8d**. The A/O-AgNP process showed lower removal for both variables.

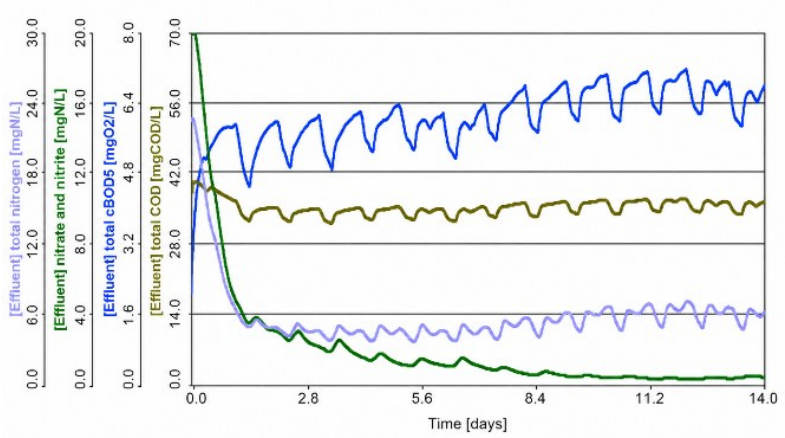

(a)

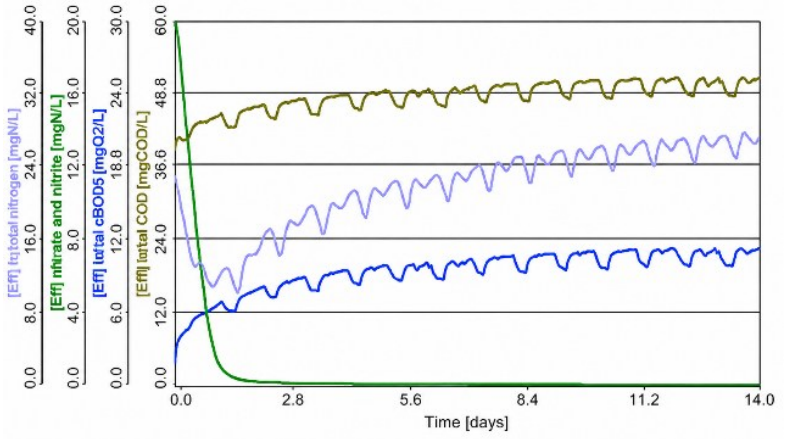

(b)

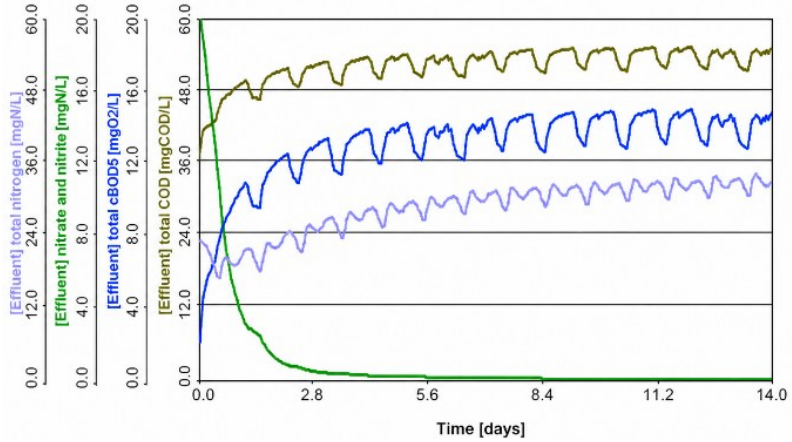

(c)

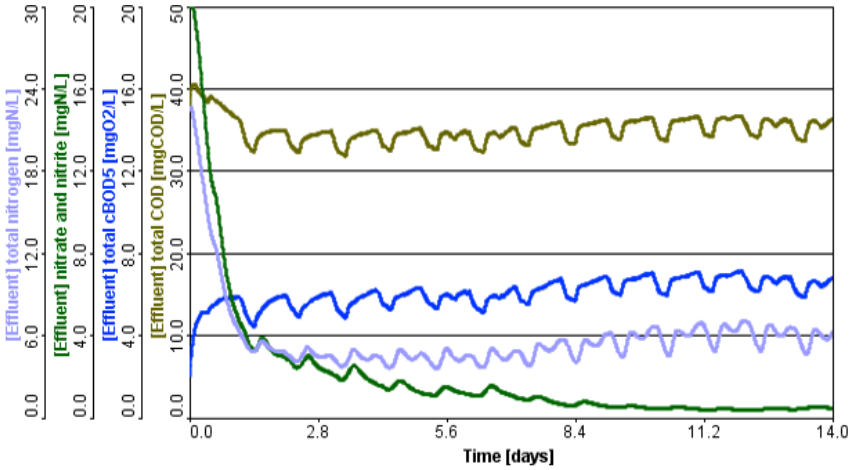

(d)

Figure 8. Effluent concentrations for dynamic conditions in the models: BSM1-AgNP (a), Bardenpho-AgNP (b), A/O-AgNP (c), and BSM1 without AgNPs as the baseline configuration (d)

For the A/O-AgNP model, the *TN* was approximately double that reported in BSM1, and the BOD_t increased by 7 times, while the COD_t remained within the range. The last two configurations thereby show that the conditions for treatment require adaptation of physical conditions and probable enhancement of stoichiometric factors. In addition, compared with the AgNP concentrations in **Figure 7**, a similar behaviour was observed, with high removal of soluble and particulate AgNP from water. Compared to previous studies, the Bardenpho and A/O configurations have been commonly used for large WWTPs, with good performance in removing carbon, nitrogen and phosphorus from wastewater **[31]**. In general, when analysing the removal portrayed by the three configurations, they achieved satisfactory results for AgNP removal, and an increase in *TN* and COD_t was noticed for two of the configurations, which, compared to the literature, can be related to the inhibition that AgNPs have on nitrogen removal in the activated sludge process **[28]**.

Table 3 presents the dynamic performance of the WWTP configurations over the last 14 days of simulation. A significant reduction in nitrogen removal efficiency was observed, particularly in the Bardenpho-AgNP and A/O-AgNP configurations, so that these configurations might require improved operational control. In contrast, *BOD* removal remains consistently high while COD removal shows moderate stability. Furthermore, the *EQI* is calculated only for steady-state conditions, as under dynamic conditions, the analysis varies over the simulation period.

Table 3. Overall results for dynamic state conditions corresponding to effluent-based removal; a dynamic *EQI* was considered outside the scope of this study

Configur-ation	*TN* [mg/L]	*TN* removal [%]	*COD* [mg/L]	*COD* removal [%]	*BOD* [mg/L]	*BOD* removal [%]	AgNP removal [%]
BSM1-AgNP	11.34	62.2	43.04	85.7	6.03	97	>81
Bardenpho-AgNP	26.68	11.1	49.83	83.4	11.18	94.4	>81
A/O-AgNP	32.2	~0	54.74	81.8	14.69	92.7	>81

In treatment performance, a reduction in removal efficiency was observed compared with the previous stage and the BSM1 baseline. **Figure 9** presents the BSM1-AgNP configuration with a *TN* removal efficiency of approximately 62%, whereas the Bardenpho-AgNP and A/O-AgNP configurations showed removal efficiencies of approximately 11%. These results might indicate

sensitivity to loading conditions, suggesting a target for implementing control strategies or operational adjustments to improve the system. In contrast, *BOD* removal was consistently above 92% across all configurations, indicating that organic matter was degraded. *COD* removal efficiencies remained between 81 to 86%, indicating a lower effect on carbon removal processes than nitrogen. Thus, dynamic operation reveals limitations in nitrogen removal, particularly in configurations with a reduced internal recirculation.

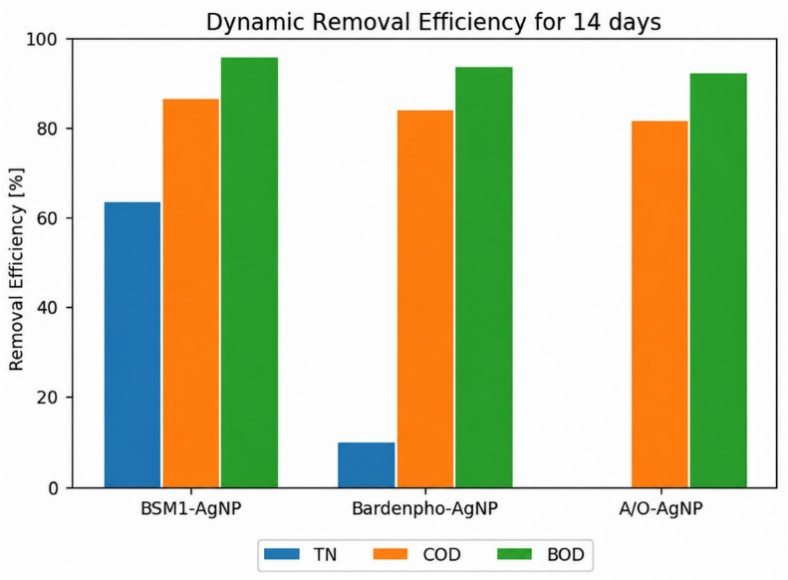

Figure 9. Removal efficiencies in the dynamic state for the BSM1-AgNP, Bardenpho-AgNP, and A/O-AgNP model

Overall, the results indicate that all configurations perform well under steady state conditions, but their behaviour under dynamic conditions differs. The BSM1 configuration shows greater robustness, which can be attributed to its higher internal recirculation and the number of reactors, given that this system is designed for nitrification-denitrification processes. Further, the Bardenpho and A/O configurations showed greater sensitivity under dynamic conditions, which is likely related to the reduced internal recycle and lower number of reactors. These differences are primarily associated with the configuration design; however, the inclusion of AgNPs may also contribute to additional inhibition effects on biological processes. Therefore, the performance strongly reflects the influence of system design and nanoparticle interactions, suggesting that WWTP configurations with higher recirculation and reactor settings may improve performance under variable loading conditions.

Although the model provides valuable insights into the behaviour and removal of AgNPs across different WWTPs, some uncertainty remains due to assumptions about influent conditions and kinetic parameters, as well as the limited availability of experimental data for model calibration. Future work could include a sensitivity analysis to evaluate the influence of key operational and model parameters on system performance, thereby improving robustness.

CONCLUSIONS AND IMPLICATIONS FOR FUTURE RESEARCH

The present study was proposed as an analytical tool for evaluating different WWTPs containing AgNPs, accounting for their fate mechanisms in wastewater and their potential for removal in wastewater treatment systems. The methodology included the design of an activated sludge model integrating adsorption-desorption, dissolution, inhibition, and chemical precipitation of AgNPs in software, and the evaluation of integrated WWTP systems. This methodology provided insight into the removal efficiency to achieve high

effluent quality. The ASM had been previously calibrated and was fully developed for the software used in this study.

Modelling of the ASM-AgNP in the software model developer showed that AgNPs can be modelled in different software, accounting for their kinetics and stoichiometry for biological treatment in WWTPs. AgNP removal was high across all configurations. When considering total mass removal, including both liquid and sludge, removal exceeded 98%. When considering only the liquid effluent, removal was approximately 82%. In terms of conventional treatment performance, *TN* removal exceeded 95% under steady state conditions, while *COD* and *BOD* removal remained above 85% and 90%, respectively. The highest effluent quality was obtained for the BSM1-AgNP model. The other two configurations showed good removal performance but exhibited inconsistent *TN* and COD_t removal, suggesting quality limitations and the need for further optimisation.

Furthermore, this area of study about emerging contaminants still needs to grow; more research is needed to increase awareness and improve understanding of nanoparticles. Although the present study considered three WWTP models incorporating AgNPs, constraints were difficult to overcome due to the limited investigation of the nanomaterial to date. For instance, more real-world WWTP data would help improve the robustness of the models; hence, more research on industry-level applications should also be incentivised. The line of investigation can be extended to include a more structured comparative analysis of AgNP dynamic data and controllers that could increase *TN* removal for the two WWTP configurations that showed inconsistencies. The models proposed in the study can further support real-world WWTPs and their operators by enabling risk evaluation, AgNPs treatment strategies, and the optimisation of performance for other emerging contaminants. By providing more information on physical conditions, reactor types, nanoparticle concentration, physical properties, fate mechanisms, removal rates, and so on, the design and monitoring of WWTPs can be enhanced over time. Moreover, a second research phase could include the development of an economic analysis to evaluate removal efficiency as a function of the NPs' concentrations entering WWTPs, to provide a deeper understanding of feasible solutions to the problem NPs pose to the environment and the world's population.

NOMENCLATURE

Symbols

$AgNP$	silver nanoparticle concentration	[mg/L]
Ag^+	silver ion concentration	[mg/L]
COD	chemical oxygen demand	[mg/L]
BOD_5	biochemical oxygen demand	[mg/L]
T	duration of evaluation	[d]
TN	total nitrogen	[mg/L]
NH_4^+-N	ammonia nitrogen concentration	[mgN/L]
NO_3^-/NO_2^-	nitrate and nitrite concentration	[mgN/L]
EQI	effluent quality index	[kg/d]
Q	influent flowrate	[m³/d]
DO	dissolved oxygen concentration	[mg/L]
SRT	sludge retention time	[d]
C_{in}	influent concentration	[mg/L]
C_{eff}	effluent concentration	[mg/L]

Subscripts and superscripts

eff	effluent
in	influent
P	particulate component
S	soluble component

Abbreviations

AgNP	Silver Nanoparticle
ASM	Activated Sludge Model
ASM-AgNP	Activated Sludge Model with Silver Nanoparticles
BSM1	Benchmark Simulation Model No. 1
WWTP	Wastewater Treatment Plant
GPS-X	Wastewater process simulation software
A/O	Anoxic/Oxic process

REFERENCES

1. V. K. Sharma, C. M. Sayes, B. Guo, S. Pillai, J. G. Parsons, C. Wang, B. Yan, and X. Ma, Interactions between silver nanoparticles and other metal nanoparticles under environmentally relevant conditions: A review, *Sci. Total Environ.*, Vol. 653, pp 1042–1051, 2019, https://doi.org/10.1016/j.scitotenv.2018.10.411.
2. P. S. Bäuerlein, E. Emke, P. Tromp, J. A. M. H. Hofman, A. Carboni, F. Schooneman, P. de Voogt, and A. P. van Wezel, Is there evidence for man-made nanoparticles in the Dutch environment?, *Sci. Total Environ.*, Vol. 576, pp 273–283, 2017, https://doi.org/10.1016/j.scitotenv.2016.09.206.
3. A. A. Keller and A. Lazareva, Predicted Releases of Engineered Nanomaterials: From Global to Regional to Local, *Environ. Sci. Technol. Lett.*, Vol. 1, No. 1, pp 65–70, 2013, https://doi.org/10.1021/ez400106t.
4. J. Pulit-Prociak and M. Banach, Silver nanoparticles - A material of the future...?, *Open Chem.*, Vol. 14, No. 1, pp 76–91, 2016, https://doi.org/10.1515/chem-2016-0005.
5. M. Noga, J. Milan, A. Frydrych, and K. Jurowski, Toxicological Aspects, Safety Assessment, and Green Toxicology of Silver Nanoparticles (AgNPs)—Critical Review: State of the Art, *Int. J. Mol. Sci.*, Vol. 24, No. 6, 2023, https://doi.org/10.3390/ijms24065133.
6. A. Y. R. Al-Assaf, M. A. Al-Katib, and A. Y. T. Al-Saffawi, The Effectiveness of Bio-Silver Nanoparticles in Treating Wastewater from the Khosar River, *Egypt. J. Aquat. Biol. Fish.*, Vol. 29, No. 3, pp 555-569, 2025, https://doi.org/10.21608/ejabf.2025.427691.
7. R. P. Pandey, A. F. Yousef, H. Alsafar, and S. W. Hasan, Surveillance, distribution, and treatment methods of antimicrobial resistance in water: A review, *Sci. Total Environ.*, Vol. 890, 164360, 2023, https://doi.org/10.1016/j.scitotenv.2023.164360.
8. R. Sharma and A. Kumar, Human health risk assessment and uncertainty analysis of silver nanoparticles in water, *Environ. Sci. Pollut. Res.*, Vol. 31, No. 9, pp 13739–13752, 2024, https://doi.org/10.1007/s11356-024-32006-9.
9. N. Rahman, M. Bharti, M. Nasir, and S. N. H. Azmi, Performance assessment of graphene oxide decorated with silver nanoparticles as adsorbent for removal of metformin from water: Equilibrium modeling, kinetic and thermodynamic studies, *Next Mater.*, Vol. 3, 100046, 2024, https://doi.org/10.1016/j.nxmate.2023.100046.
10. M. Baalousha, Y. Yang, M. E. Vance, B. P. Colman, S. McNeal, J. Xu, J. Blaszczak, M. Steele, E. Bernhardt, and M. F. Hochella, Outdoor urban nanomaterials: The emergence of a new, integrated, and critical field of study, *Sci. Total Environ.*, Vol. 557–558, pp 740–753, 2016, https://doi.org/10.1016/j.scitotenv.2016.03.132.
11. S. Zaheer Ud Din, K. Shah, N. Bibi, H. H. Mahboub, and M. A. Kakakhel, Recent Insights into the Silver Nanomaterials: an Overview of Their Transformation in the Food Webs and Toxicity in the Aquatic Ecosystem, *Water, Air, Soil Pollut.*, Vol. 234, No. 2, 114, 2023, https://doi.org/10.1007/s11270-023-06134-w.
12. L. Li, G. Hartmann, M. Döblinger, and M. Schuster, Quantification of nanoscale silver

particles removal and release from municipal wastewater treatment plants in Germany, *Environ. Sci. Technol.*, Vol. 47, No. 13, pp 7317–7323, 2013, https://doi.org/10.1021/es3041658.

13. K. Ganguly, S. D. Dutta, D. K. Patel, and K. T. Lim, Silver nanoparticles for wastewater treatment, in *Aquananotechnology: Applications of Nanomaterials for Water Purification*, Amsterdam, Netherlands: Elsevier, 2020, pp 385–401, https://doi.org/10.1016/B978-0-12-821141-0.00016-1.
14. H. X. Shi, S. Y. Liu, J. S. Guo, F. Fang, Y. P. Chen, and P. Yan, Potential role of AgNPs within wastewater in deteriorating sludge floc structure and settleability during activated sludge process: Filamentous bacteria and quorum sensing, *J. Environ. Manage.*, Vol. 349, 119536, 2024, https://doi.org/10.1016/j.jenvman.2023.119536.
15. A. Grosser, A. Grobelak, A. Rorat, P. Courtois, F. Vandenbulcke, S. Lemière, R. Guyoneaud, E. Attard, and P. Celary, Effects of silver nanoparticles on performance of anaerobic digestion of sewage sludge and associated microbial communities, *Renew. Energy*, Vol. 171, pp 1014–1025, 2021, https://doi.org/10.1016/j.renene.2021.02.127.
16. M. Henze, W. Gujer, T. Mino, and M.C.M. van Loosedrecht, Activated Sludge Models ASM1, ASM2, ASM2d and ASM3, Report, Lund University and IWA Taskgroup on Benchmarking of Control Strategies for WWTPs, London, UK, 2000. https://doi.org/10.2166/9781780402369.
17. K. V. Gernaey, M. C. M. Van Loosdrecht, M. Henze, M. Lind, and S. B. Jørgensen, Activated sludge wastewater treatment plant modelling and simulation: State of the art, *Environ. Model. Softw.*, Vol. 19, No. 9, pp 763–783, 2004, https://doi.org/10.1016/j.envsoft.2003.03.005.
18. J. Alex, L. Benedetti, J. Copp, K. V. Gernaey, U. Jeppsson, I. Nopens, M. Pons, L. Rieger, C. Rosen, J. P. Steyer, P. Vanrolleghem, and S. Winkler, Benchmark Simulation Model No. 1 (BSM1), Report, LUTEDX/(TEIE-7229)/1-62, Lund University and IWA Taskgroup on Benchmarking of Control Strategies for WWTPs, Lund, Sweden, 2008.
19. X. Wu, Y. Yang, G. Wu, J. Mao, and T. Zhou, Simulation and optimization of a coking wastewater biological treatment process by activated sludge models (ASM), *J. Environ. Manage.*, Vol. 165, pp 235–242, 2016, https://doi.org/10.1016/j.jenvman.2015.09.041.
20. Y. Tian, Z. Hu, H. Cheng, J. Xiao, and L. Wu, Process Modeling and Its Application in Municipal Wastewater Treatment Plant Based on Seasonal Temperature Variations: A Case Study in Eastern China, *Water (Switzerland)*, Vol. 17, No. 7, pp 1–18, 2025, https://doi.org/10.3390/w17070994.
21. Y. Zhu, H. Zhang, H. Sun, Y. Zhang, L. Yang, C. Liu, X. Yang, and Y. Liu, Effect of silver nanoparticles on biological nitrogen removal in sequential batch wastewater treatment process: Microbial communities, functional genes, and interactions, *J. Water Process Eng.*, Vol. 70, 2025, https://doi.org/10.1016/j.jwpe.2025.107114.
22. Z. Fan, Y. Huang, Y. Duan, Z. Tang, and X. Yang, Effects of silver nanoparticles and various forms of silver on nitrogen removal by the denitrifier Pseudomonas stutzeri and their toxicity mechanisms, *Ecotoxicol. Environ. Saf.*, Vol. 269, 115785, 2024, https://doi.org/10.1016/j.ecoenv.2023.115785.
23. Y. Guo, N. Cichocki, F. Schattenberg, R. Geffers, H. Harms, and S. Müller, AgNPs change microbial community structures of wastewater, *Front. Microbiol.*, Vol. 10, pp 1–12, 2019, https://doi.org/10.3389/fmicb.2018.03211.
24. L. Chen, W. Feng, J. Fan, K. Zhang, and Z. Gu, Removal of silver nanoparticles in aqueous solution by activated sludge: Mechanism and characteristics, *Sci. Total Environ.*, Vol. 711, 135155, 2020, https://doi.org/10.1016/j.scitotenv.2019.135155.
25. H. Yu, H. Zhang, C. Zhang, R. Wang, S. Liu, R. Du, and W. Sun, Advances in treatment technologies for silver-containing wastewater, *Chem. Eng. J.*, Vol. 496, 153689, 2024,

https://doi.org/10.1016/j.cej.2024.153689.
26. P. Vilela, H. Liu, S. C. Lee, S. Hwangbo, K. J. Nam, and C. K. Yoo, A systematic approach of removal mechanisms, control and optimization of silver nanoparticle in wastewater treatment plants, *Sci. Total Environ.*, Vol. 633, pp 989–998, 2018, https://doi.org/10.1016/j.scitotenv.2018.03.247.
27. F. Fu and Q. Wang, Removal of heavy metal ions from wastewaters: A review, *J. Environ. Manage.*, Vol. 92, No. 3, pp 407–418, 2011, https://doi.org/10.1016/j.jenvman.2010.11.011.
28. P. Cervantes-Avilés, Y. Huang, and A. A. Keller, Incidence and persistence of silver nanoparticles throughout the wastewater treatment process, *Water Res.*, Vol. 156, pp 188–198, 2019, https://doi.org/10.1016/j.watres.2019.03.031.
29. Hydromantis, GPS-X Technical Reference, Technical Report, Hydromantis Environmental Software Solutions, Inc., Hamilton, Ontario, Canada, 2017.
30. Hydromantis, GPS-X Model Developer Guide, Technical Report, Hydromantis Environmental Software Solutions, Inc., Hamilton, Ontario, Canada, 2019.
31. M. S. Kadri, R. R. Singhania, D. Haldar, A. K. Patel, S. K. Bhatia, G. Saratale, B. Parameswaran, and J. S. Chang, Advances in Algomics technology: Application in wastewater treatment and biofuel production, *Bioresour. Technol.*, Vol. 387, 129636, 2023, https://doi.org/10.1016/j.biortech.2023.129636.

Paper submitted: 20.12.2025
Paper revised: 09.05.2026
Paper accepted: 13.05.2026